1 Abstract

It is shown moreover that the crude method of matching the UXO against templates is more reliable than a Bayesian appraoch, but that a Bayesian approach can be used in concert with PCM to modestly improve the already excellent performance of PCM.

2 Introduction

A key problem in remediation of domestic Department of Defense sites contaminated with unexploded ordnance (UXO) is classification of buried anomalies as either UXO or scrap metal. The problem of anomaly detection has been mostly solved on land through the use of magnetometers and electromagnetic induction (EMI) sensors [Nelson et al., 2003] however, detection methods do not discriminate between dangerous UXO and harmless scrap metal. The classification problem fractures into several categories, depending on the type of instrument (time or frequency domain EMI, magnetometer, GPR etc.), the type of UXO, and the spatial distribution of anomalies, e.g. single or multiple objects. The algorithm discussed here considers only time domain EMI data recorded over single objects. While the lone object problem may not always represent the real-world, any classification algorithm which cannot solve this problem, is unlikely to succeed in more complicated situations. Since reliable classification of single objects remains an open problem, it is addressed first.

Intact UXO have the property of rotational symmetry about one axis, and furthermore, UXO tend to be furthen extended along the axis of rotational symmetry by an aspect ratio of around four or five. Induced currents in these objects circulate primarily about the long axis, and less so in the other directions. For over a decade researchers in the field of UXO detection and discrimination have been working with physics-based models approximating subsurface conductors by induced magnetic dipoles. Decaying currents in the target are represented by an induced dipole moment tensor ($\mathbf{M}$). Determination of $\mathbf{M}$ is the objective of most UXO EMI inversion algorithms. Diagonalizing $\mathbf{M}$ yields dipole-moment amplitudes in the principle directions. The time dependent relationship between these moment amplitudes is the chief source of information regarding target shape and aspect ratio. Early attempts to exploit this information such as [Khadr et al., 1998] and [Pasion and Oldenburg, 2001] looked promising, but in the decade since their publication no comprehensive solution to the target identification problem has emerged. A 2004 report on EMI methods for UXO discrimination [Butler, 2004] emphasizes the need for cooperation between the techniques of UXO detection and classification which were at the time state of the art. The techniques discussed were magnetometery, time and frequency domain EMI (although the UXO problem may require incorporating GPR and acoustic methods for some cases). Some work incorporating magnetometery and TDEM is being explored ([Pasion et al., 2008]) but this is not currently the standard methodology. [Butler, 2004] concluded that most existing methods were producing similar results and that various noise sources including

geologic, position uncertainty, and instrument noise were the main factors impeding progress.

Since 2004 significant work has been conducted with time domain multiple-transmitter, multiple-receiver (MTMR) systems, in both theoretical modeling and instrument design, specifically [Smith and Morrison, 2005], [Smith et al., 2007]. The new generation of MTMR systems, of which BUD is an example, has increased the efficiency of surveying by enabling array-style acquisition and processing to be employed with a single instrument sounding. The EM data from an array measurement carries information about the shape/size/composition of the subsurface scatterer, and the three-component illumination of the target allows superior determination of aspect ratio as was previously possible. Recent field surveys using the BUD system suggest that object classification is possible based on information extracted from a surface measurement, e.g. [Gasperikova et al., 2009]. Time-dependent polarizability tensors obtained via data inversion under the assumption that a lone isolated spheroid is the source of receiver deviation from noise,([Smith et al., 2007]) were examined by [Kappler, 2008] for the Camp Sibert AL dataset. [Kappler, 2008] employed the technique of *Polarizability Curve Matching* (PCM). The method was applied to 416 *cued* and *OpenField* measurements. 99 of these were classified as UXO and the remaining 315 as scrap/clutter. The routine yielded 0 false negatives **FN**, and only 5 false positives **FP** however, the anomalies at Camp Sibert were typically large, and the scrap were typically small. Thus, most of the classification was done easily depending on the amplitude of the polarizability curves associated with the anomalies. The PCM method of is a

pattern classifier which treats as the domain, the three polarizability curves output by an inversion algorithm ([Smith and Morrison, 2004]. This method is extended here to the Yuma, AZ BUD survey, where data were acquired over a Calibration Grid (CG) and a Blind Test Grid (BTG). It is shown that an augmented form of the PCM approach can succeed when multiple UXO are present, even when the UXO targets span a wide range of sizes, and can easily be smaller than the scrap. When many different types of object are present, PCM is shown to have a dramatic effect in generating so-called 'diglists' which order anomalies by priority of extraction from the ground.

The underlying idea of the PCM method is that UXO of a particular class tend to have nearly invariant PC representations (see Figure 1) over a wide range of depths. By forming a set of training curves from data acquired over known objects, field data can be compared to the training data, and the class of object beneath the system can be determined by identifying a matching template from the training data. After examining hundreds of P-curve printouts on loglog scale where known targets were placed beneath the BUD system, in most cases it is an easy matter to decide the class of an object by comparing the P-curves against a collection of templates. PCM is simply a computer algorithm which extends this supervised method to an unsupervised method which emulates the human interpretters decisions. [Pasion et al., 2007] also applies a method based on training data (libraries) with encouraging results, although some munitions are occasionally misclassified as other munitions. It is important to note that [Pasion et al., 2007] takes as input only data acquired over UXO, and the range of the classifica-

tion algorithm consists only of UXO. The problem of saving costly digging, is not to distinguish between various dangerous objects, but to distinguish between objects which are dangerous and those which are not.

An ideal classification method is a map between sets. Elements of the domain $\mathcal{X}$ are themselves sets, comprising data acquired by one or more field instruments, together with the meta-data regarding those instruments, and information about ambient conditions, such as meteorologic, and geologic data, as well as noise measurements. The range is the collection of categories relevant to the classification problem, thus for UXO, the range partitions into two sets; Dangerous $\mathbf{D}$=$\{$data soundings for which a UXO is present$\}$, and Benign $\mathbf{B}$=$\{$data soundings for which no UXO are present$\}$. The UXO-present set $\mathbf{D}$ is itself partitioned into a set of subclasses, one for each type of munition. The method described here is not designed to map each element of $\mathcal{X}$ to a unique subclass, but rather it assigns a pseudoprobability to each x in $\mathcal{X}$, that the data are associated with a particular type of object. The specific form of f developed here compares field data soundings against soundings from a training dataset $\mathcal{T}$ which are acquired over known targets. Thus, the object classes in the range of f are dictated by the classes represented in $\mathcal{T}$, hence the function f depends in part on the reference training dataset.

In practice classification may be complicated. Consider for example the case of data acquired with a UXO near the system, but too far away to get reasonable SNR. How do we classify this situation? It depends on the volume of subsurface which the operator is confidently interrogating. This sort of ambiguity can be mitigated by constraining the space of estimated object

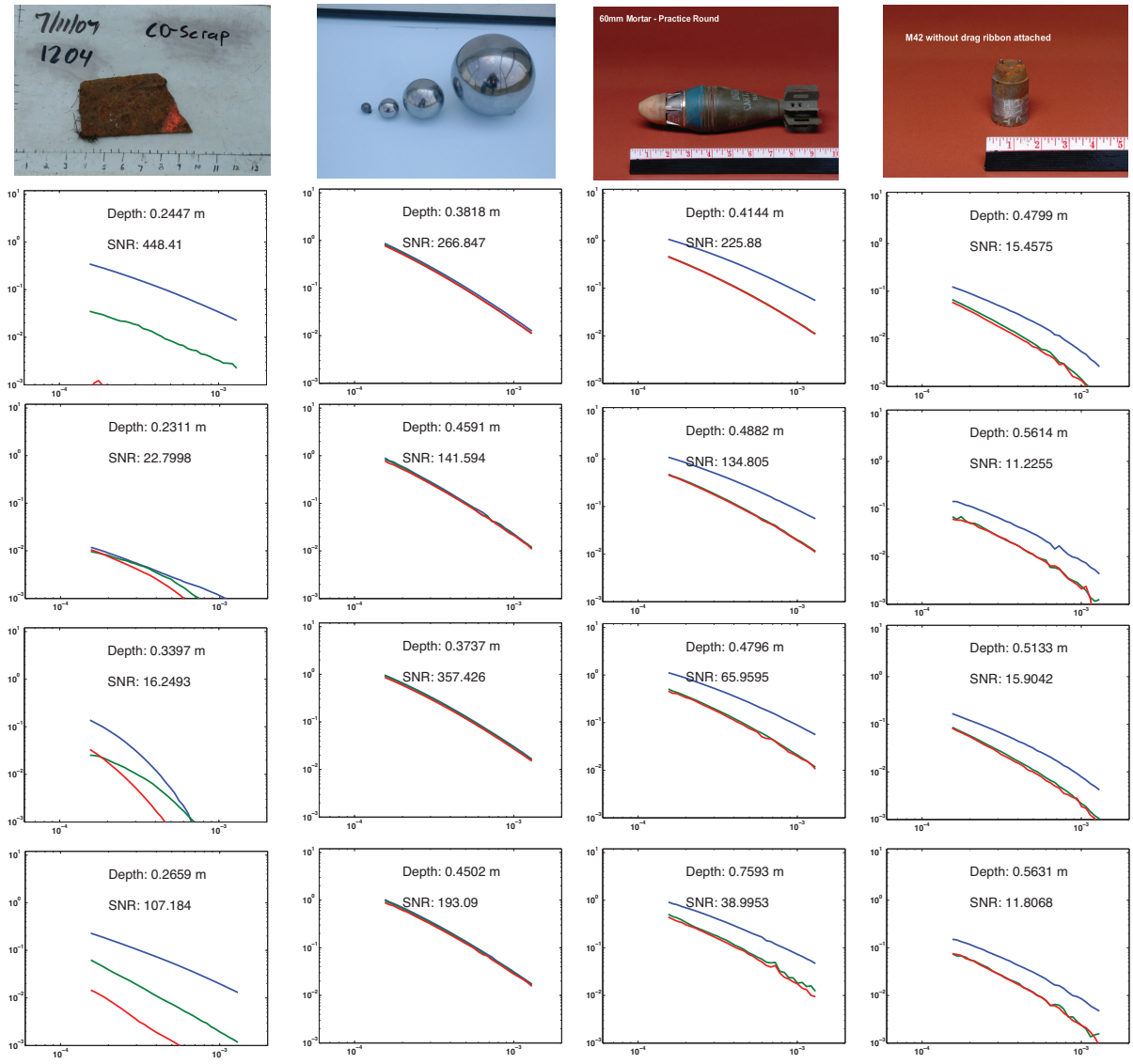

Figure 1: Collection of PCs from various targets motivating the curvematching method of identification.

positions, and SNR levels which are admitted as inputs to the classification function. Further complicating the situation are uncertainties in the position and characteristics of instrument coils, and fluctuations in ambient and geologic noise which can lead to non-unique inversion results. This problem tends to abate as more constraints are forced on the interpretation by multiple receivers operating simultaneously. In the case of BUD, eight channels record data, and the position of the recievers with respect to the transmitters are fixed to a high degree of accuracy.

The following assumptions are made:

1. There is at most one object present within the detection footprint of the system.

2. Placing a data sounding into the set **B** means that there is no object of diameter greater than d at depths shallower than $z_d(d)$, as defined by the depth-to-10%-uncertainty curves, as shown in [Morrison et al., 2005].

3. SNR of a data sounding admitted to classification is greater than a threshold value.

This manuscript is organized as follows: The dataset treated here, including preprocessing are described in section XX1. This includes a subesection on criteria for sorting data into two sets, those that are admissible to PCM and those that will be classified as *Can't Analyse*. The underlying idea of the PCM approach is mathematically formalized in section XX2. A brief disucussion of Bayesian classifiers is included in section XX2 along with a description of how this classifier can be applied to refine PCM. Section XX3

gives results from the simplest PCM method, as well as from PCM augmented with techniques of voting, subclass consideration, and a Bayesian classifier. Results of the cross validation trials are discussed in section XX4, together with a plan for applying the method the the BTG dataset. In section XX5 preliminary conclusions are offered without scoring results from BTG, which will be presented at SAGEEP 2011.

3 PREPROCESSING AND SORTING

Static BUD data are acquired by positioning the system over an area of interest and engaging the onboard data acquisition system. A single field measurement comprises recordings from 8 differenced-pair receivers, together with Tx Current waveforms from each of three orthogonal transmitters. Such a measurement includes 320 stacked records for each Tx which are acquired over a period of 2s. All cycling between tranmitters and synchronization of channels is automatically handled by the system electronics. Prior to calculation of principal polarizabilities the Rx responses are differenced against a "Background" measurement. The collection of raw data, background measurement, and metadata regarding instrument or background noise phenomena are referred to en masse as a *sounding*. An inversion program which calculates polarizability curves ([Smith and Morrison, 2004]), is used to map each sounding to a set of three polarizability curves. These are represented by three vectors of length 34, $\mathbf{p}_1, \mathbf{p}_2$, and $\mathbf{p}_3$ where the subscript 1 is the polarizbility with the largest eignvalue, and subscript 3 denotes the lowest eigenvalue. The 34 logarithmically-spaced time gates are the same for all three curves, and

for all soundings. We will sometimes refer to the 'raw'polarizability curves from sounding x as $P(x)$.

The polarizability curves from hundreds of BUD soundings taken at the YUMA Calibration Grid, together with some scrap soundings from the Camp Sibert, AL survey were compiled into master dataset (or universe) $\mathcal{U}$. $\mathcal{U}$ is the union over M=(29) disjoint sets $S_i, i = 1..M$ where each class is comprised of example soundings over a particular class of target.

$$\mathcal{U} = \bigcup_{i=1}^{M} S_i \tag{1}$$

Each sounding in this set is examined to see if it is fit for PCM analysis. It is obvious when visually inspecting the data that poor classification can be expected if soundings are kept which have very poor SNR, and/or unrealistic depth estimates. The BUD system specifications do not provide for discrimination of targets buried deeper than 1m (although the do detect these objects) and data with SNR less than 2 are removed from the set $\mathcal{U}$ before any further processing takes place. In practice, detected objects with low SNR can be dealt with as provided in the discusion. All admitted curves are 'paper-projected', and replaced with quadratic fits before PCM is run.

3.1 Paper Projection

In an effort to approximate the method of comparing printouts, the Pcurve coordinates are log-transformed and scaled to a set of linear coordinates that the curves would have, if a cartesian grid were laid on top of a loglog printout on an 8.5 x 11 sheet of paper. Given a set of loglog axes with y axes limits

$[y_1^L, y_2^L]$, and xaxes limits $[x_1^L, x_2^L]$, and an overlain linear axes with the origin in the bottom left of the sheet, with linear y-axes limits [0,y_2], and x-axes limits [0,x_2], a point (x,y) is transformed to (x',y') according to:

$$y' = \frac{y_2 log_{10}(\frac{y}{y_1^L})}{log_{10}(\frac{y_2^L}{y_1^L})} \tag{2}$$

$$x' = \frac{x_2 log_{10}(\frac{x}{x_1^L})}{log_{10}(\frac{x_2^L}{x_1^L})} \tag{3}$$

which, when using an 8.5 x 11 sheet on the axes shown in the example Figure, results in scaling each of the $\mathbf{p}_i$:

$$\mathbf{p'}_i = \frac{11 log_{10}(\frac{\mathbf{p}_i}{1e-3})}{4.027} \tag{4}$$

$$\mathbf{t}' = \frac{8.5 log_{10}(\frac{\mathbf{t}}{6e-5})}{1.523} \tag{5}$$

3.2 Quadratic Curve Fitting

The projected polarizability values $\mathbf{p'}_i$ together with the projected time gates $\mathbf{t}'$ are the base quantities used in the curve matching method. Each $\mathbf{p'}_i$ is further condensed to a second order polynomial approximation by least-squares fitting a quadratic to $\mathbf{p'}_i$ vs. $\mathbf{t}'$. Thus for each p-curve $\mathbf{p'}_i$, we obtain three quadratic curve fit coefficients A_i, B_i, C_i. The quadratic approximation to $\mathbf{p'}_i$, we will call $\mathbf{q}_i$. The curve $\mathbf{q}_i$ is plotted vs $\mathbf{t}'$ by the relation:

$$\mathbf{q}_i(t') = A_i t'^2 + B_i t' + C_i. \tag{6}$$

In most cases, $\mathbf{p'}_i$, and $\mathbf{q}_i$ are indistiguishable by eye, however when SNR is low, $\mathbf{p'}_i$ can take on a jagged character which cannot be well fit by a second order polynomial. The three quadratic fit curves, each of length 34 are finally concatenated into a single vector of length 102 for easier manipulation in programing. The 102-length quadratic fit represetnatation of a sounding x will be referred to as $\mathbf{Q}(\mathbf{x})$

4 PCM ALGORITHM

The composition of the universe $\mathcal{U}$ obtained from the CG and Sibert data is shown in Table 1. Before applying the method to field data, an extensive series of cross-validation experiments on this dataset of soundings from known targets.

To perform a single cross validation trial, $\mathcal{U}$ is partitioned into two disjoint sets; $\mathcal{U} = \mathcal{T} \cup \mathcal{F}$. The set $\mathcal{T}$ acts as a training library, and the second set $\mathcal{F} = \mathcal{U}/\mathcal{T}$ acts as a mock field dataset. $\mathcal{T}$ is the union $\cup_{i=1}^{M} \mathbf{T}_i$ where $\mathbf{T}_i$ is generated by selecting at random either 1,2, or 3 elements from each of the S_i according to the following rule: if there are fewer than 5 elements in S_i, then ${}^{\#}\mathbf{T}_i = 1$, if there are between 5 and 15 elements in S_i, then ${}^{\#}\mathbf{T}_i = 2$, and if there are more than 15 elements in S_i, then ${}^{\#}\mathbf{T}_i = 3$.

The actual classification process is quite crude and straightforward. For

a given field sounding x in $\mathcal{F}$, a single cross-validation trial returns a class which the sounding was determined to be nearest to in the sense that of all the trianing data, the training curves which were nearest x in a least squares sense are assumed to be representative of the class of which x is a member.

Preliminary results from cross validation indicated that most soundings are classified correctly, but some are not. Sometimes a given sounding is classified differently depending on the chosen training data. In order to deal with the non-unique results, I apply a voting scheme; By running the xVal algorithm on each element of F with many (say 150) training data configurations, each xVal is taken as a vote for the class of the sounding. In this case, the object is classed finally as the type which receives the most votes.

The PCM method returns a class which F probably belongs to, as well as a pseudo-probability that the classification is accurate.

Sometimes a given sounding is classified differently depending on the chosen training data. In order to deal with the non-unique results, I apply a voting scheme; By running the xVal algorithm on each element of F with many (say 150) training data configurations, each xVal is taken as a vote for the class of the sounding. In this case, the object is classed finally as the type which receives the most votes.

5 RESULTS

SIMPLEPCM Preliminary trials using this method showed encouraging results, AVGNUMBER FN and FP... for CULLED TRG DATASET Of 336 objects being classified, cross validation (XV) yielded on average 5 false negatives and 33 false positives when object classification is considered between the set of dangerous and benign objects only. This statistic is slightly misleading because incorrect classifications were not uniformly distributed amongst the XV runs. Figure **??** shows the number of false negatives encountered in 100 XV runs, and shows that approximately two-thirds of the time, no FPs are encountered at all. In rare cases eight FNs are encountered. This inconsistent success is attributed to some scrap objects which "look" somewhat like UXO. Such occasional failures can be mitigated by running the algorithm multiple times, with slightly different training data for each run. A dig-list is then generated using a voting scheme, where objects are ordered by the frequency with which they are classed as dangerous.

IMPROVED PCM ALGORITHM using VOTING, SUBCLASSES, and BAYESIAN feature classifier

DISCUSSION

5.1 BAYESIAN REFINEMENTS

Preliminary work with purely feature-based classification yields encouraging results (ROC curves comparable in shape to the voting method), but there are also some problems with the method, namely the limited number of training data for some categories. Implemetation of multidimensional Bayesian

classifiers requires inverting the feature-data-covariance matrix. These matrices can become ill-conditioned in the case where the number of training samples is on the order of the number of features (N) which is the same as the dimension of the covariance matrix. Similar problems are also encountered when features are highly correlated, i.e. the dimensions of the feature vector are not independent. These problems will be examined in more detail later. For now, we note that you need at least as many examples in a training set as there are features, as the dimension of the $N \times N$ covariance matrix is the same as the number of features N, and an $N \times N$ covariance matrix will span at most the dimension of the number of obserations used in calcualting it. The collection of features under current study are listed below:

1. **P11**: Amplitude of the primary polarizability in the first time gate.

2. **D23**: Integrated measure of the difference between the second and third polarizability curves, a.k.a. primary axial symmetery parameter

3. **D12**: Integrated measure of the difference between the second and third polarizability curves, a.k.a. secondart axial "diskness" parameter

4. **M1**: The slope of a straight line fit to the primary polarizability in logspace

5. **K1**: The Curvature of the primary polarizability in log space $Derivetheequationfortheradi$ $(1+f'(x)^2)(3/2)/f''(x), wherexisthexcoordinateforapointonthecurve, f'(x)isthefirstderiv$

6. **P_INDEX**: Integrated measure of the amplitude of all P-curves, witha time factor

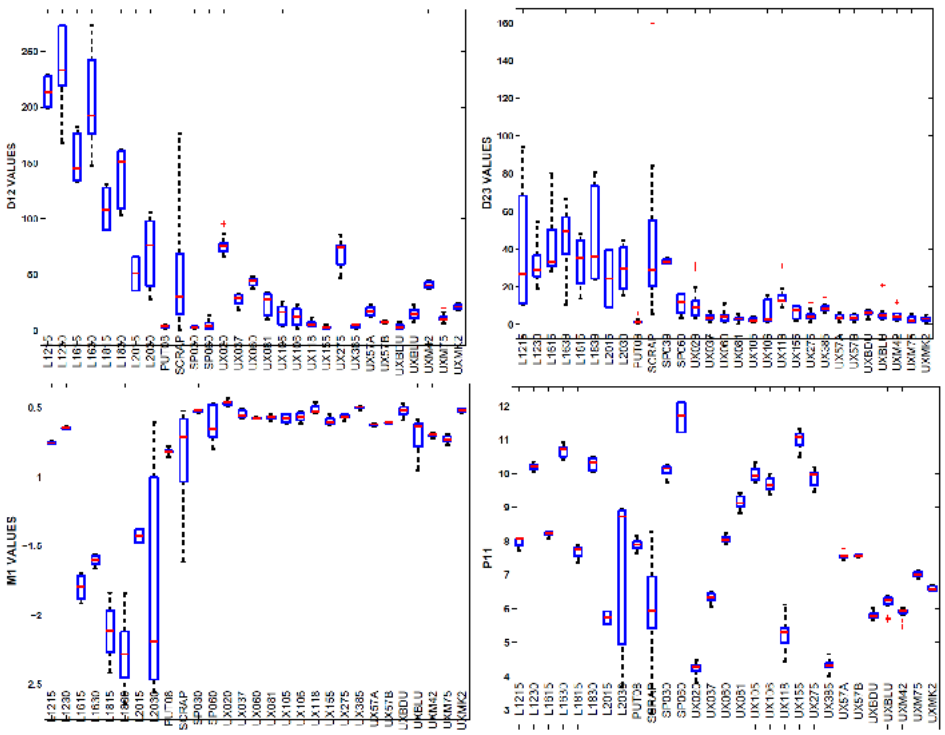

Figure 2: bw

7. **Median Residual**: Median best-fit residual comparing the sounding to a particular class during voting.

Several of these features are shown as box-and-whisker plots in Figures XX-YY. In each boxplot, the red line is the median, and the interquartile range is specified by the box edges. The Whisker lines represent the maximum, and minimum values obtained by the data, but whiskers are not allowed to exceed 1.5 times the length of the box. Points lying outside the whiskers are denoted by the red crosses.

I have developed the concept of **Classes of Limited Distinguishability**. These classes, for example {UX155 vs. SP060}, or {UX105 vs. UX106}, or {UX081 vs. UX275} are not so easily sorted using simple PCM as devel-

oped here. Usually, items are classified correctly, but after running several thousand trials, we can get a feeling for the emprical distribution of errors inhernt in the voting scheme. From these statisitcs we can identify the true set of classes of which an sounding may be a member. The matlab script identifyConfusionClasses.m works in the following way; for each subclass, the voteRecord is scanned, and a list of all object MUIDs which received some votes for that subclass are identified. Then, the TRUE classes of each of these MUIDs objects are recorded as the CLD(subclass). The resultant list is an indicator, that, "Say object X is classified, in part as subclass S. Then we admit in feature space, CLD(S) as possible ellipsoids to consider. If object X is classed as S1, S2, ...SN, then we admit as ellipsods UNION(CSP(S1), CSP(S2), ...CSP(SN)).

5.2 CROSS VALIDATION RESULTS

SIMPLE PCM APPLIED TO THE TRAINING DATA RESULTS IN FIGS 3 and 4.

5.2.1 SUBCLASS REFINEMENTS

It is sometimes the case that a particular target can yield different responses such as those shown for a 57mm target in Figure 5. The relationship between object-system orientation is not clear if it exists that causes these variations. UX57 for example come in Flavor A and B. What can happen is that trg data can by random chance be drawn all of type A or all of type B. This can

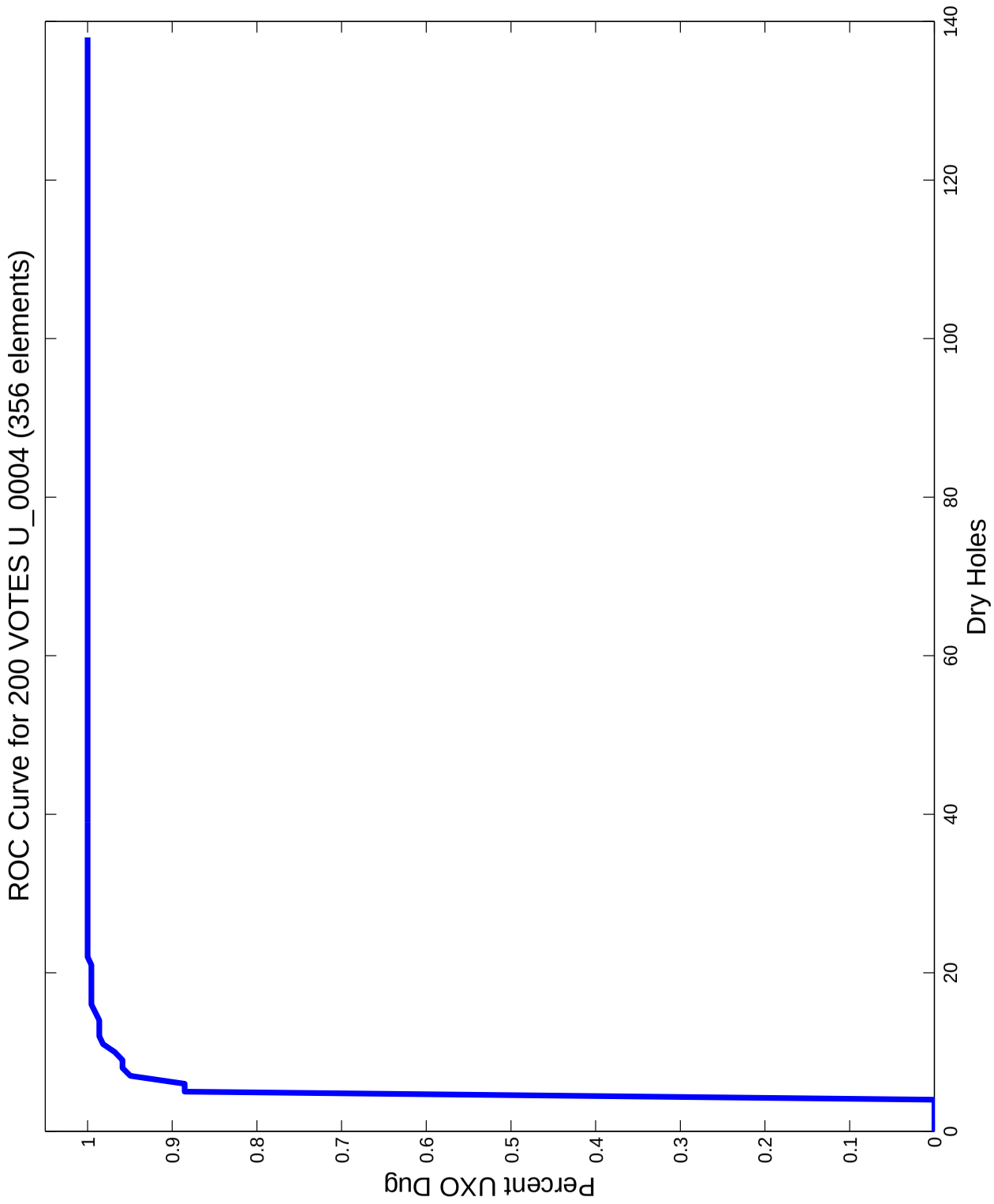

Figure 3: reliableROC

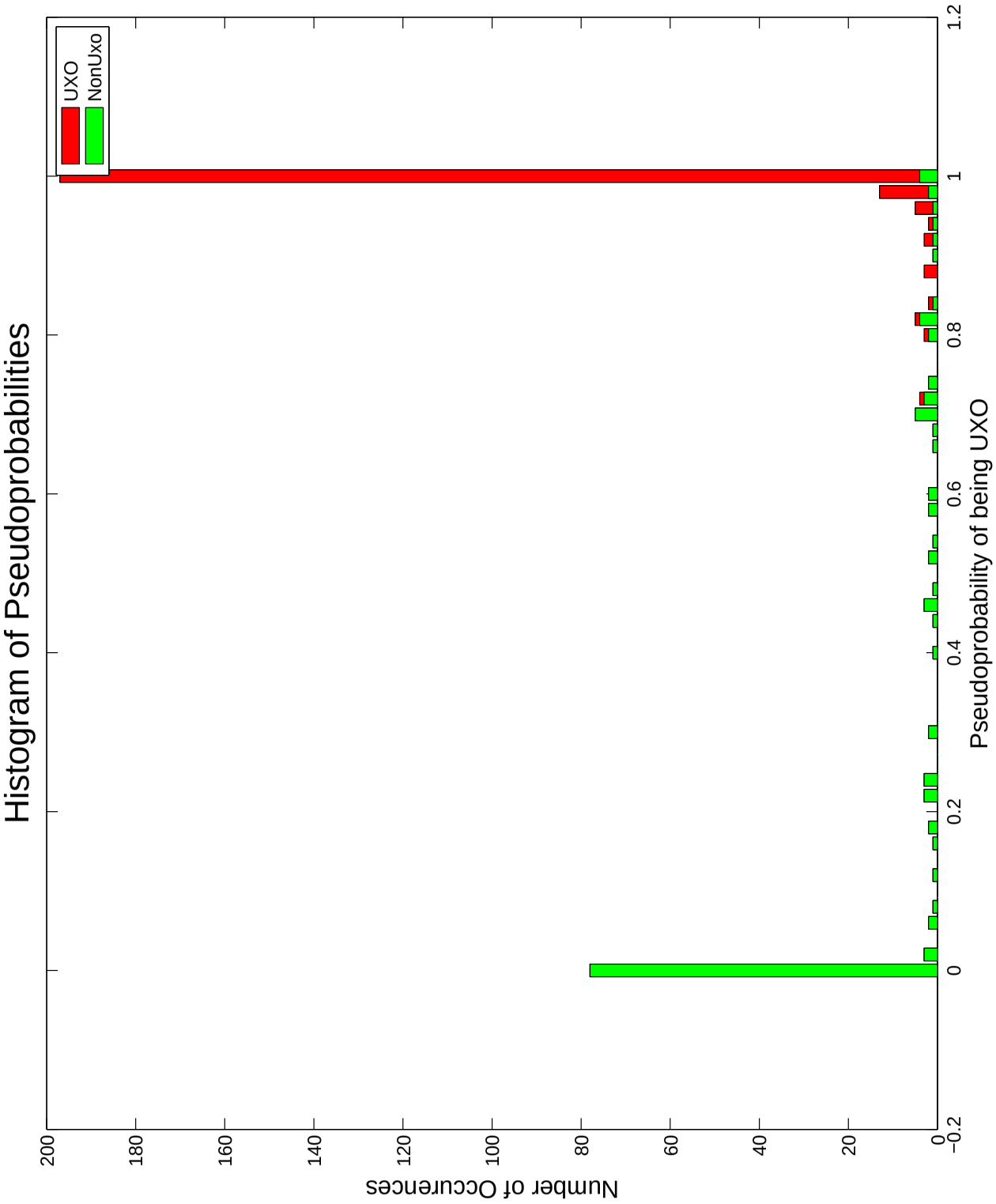

Figure 4: Reliable PseudoProb

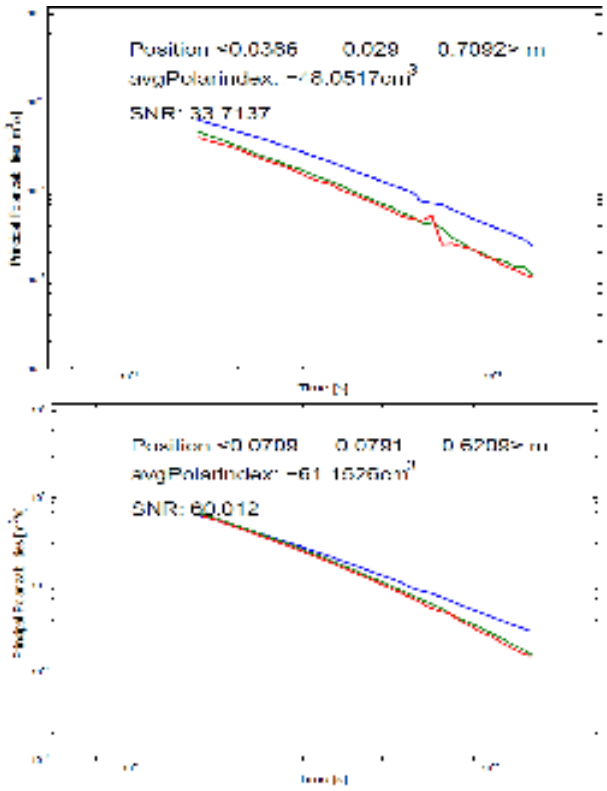

Figure 5: ux57ab

lead to misclassification. Although over many votes the object still classes as 57mm, it doesn;t get as many votes as it could. This led me to cut classes like this into subclasses, and insist that at least one example per subclass went into the trg data. Doing this with 57mm sginificantly raised the lowest RED vote from around 70 to around 85 percent.

Applying these refinements gives PCM results shown in Figure

5.2.2 BAYESIAN METHOD

Using simple Bayes on P11, D23, M11, D12, a 4-dimensioanl feature, we get Figurs 7 and 8. Distributions of the Probability are more bimodal than

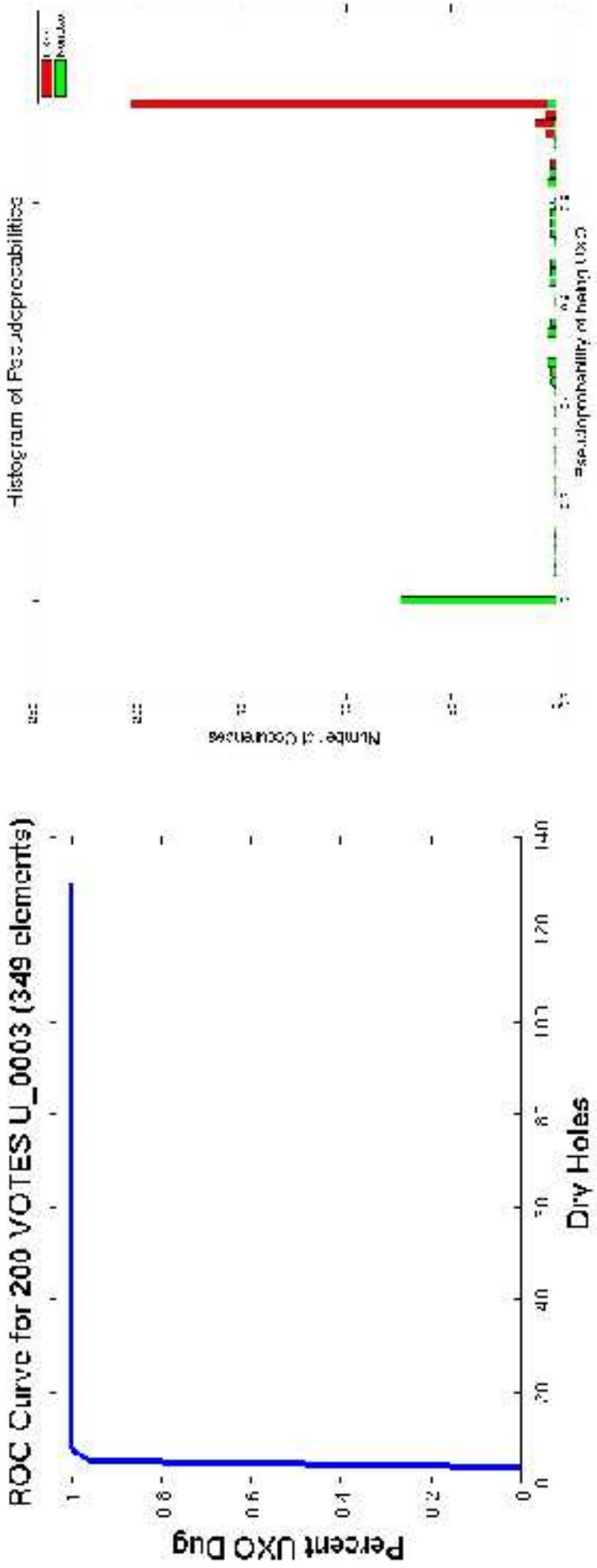

Figure 6: rh57

for the Pseudoproabability, but we see that False Neagatives Occur in the Bayesian method.

5.2.3 HYBRID

A modest improvement to the PCM results can be achieved if the diglist is ordered as follows: Run PCM, then run BAYES. In cases where both methods say with better than some threshold (i used 90%) on the type of object... then place the object at top or bottom of list accordign to **D** or **B** classification. The remaining objects are ordered as per PCM and inserted between the confident scrap plus confident UXO.

6 Application of modified PCM to YUMA Blind Test Grid

The Yuma BTG data set will be formatted for input to the 'Augmented PCM' and the results of the classification will be sent to the sponsor for scoring along with a summary report describing the APCM approach.

7 DISCUSSION

7.1 FutureWork

Consider sounding UID=130. This scrap object pictured in Figure: 10.

is voted 100% of the time as a 37mm (PCM), BUT, its residual is around 15. Typical intraclass Residuals for 37mm are around 1. Probably with a

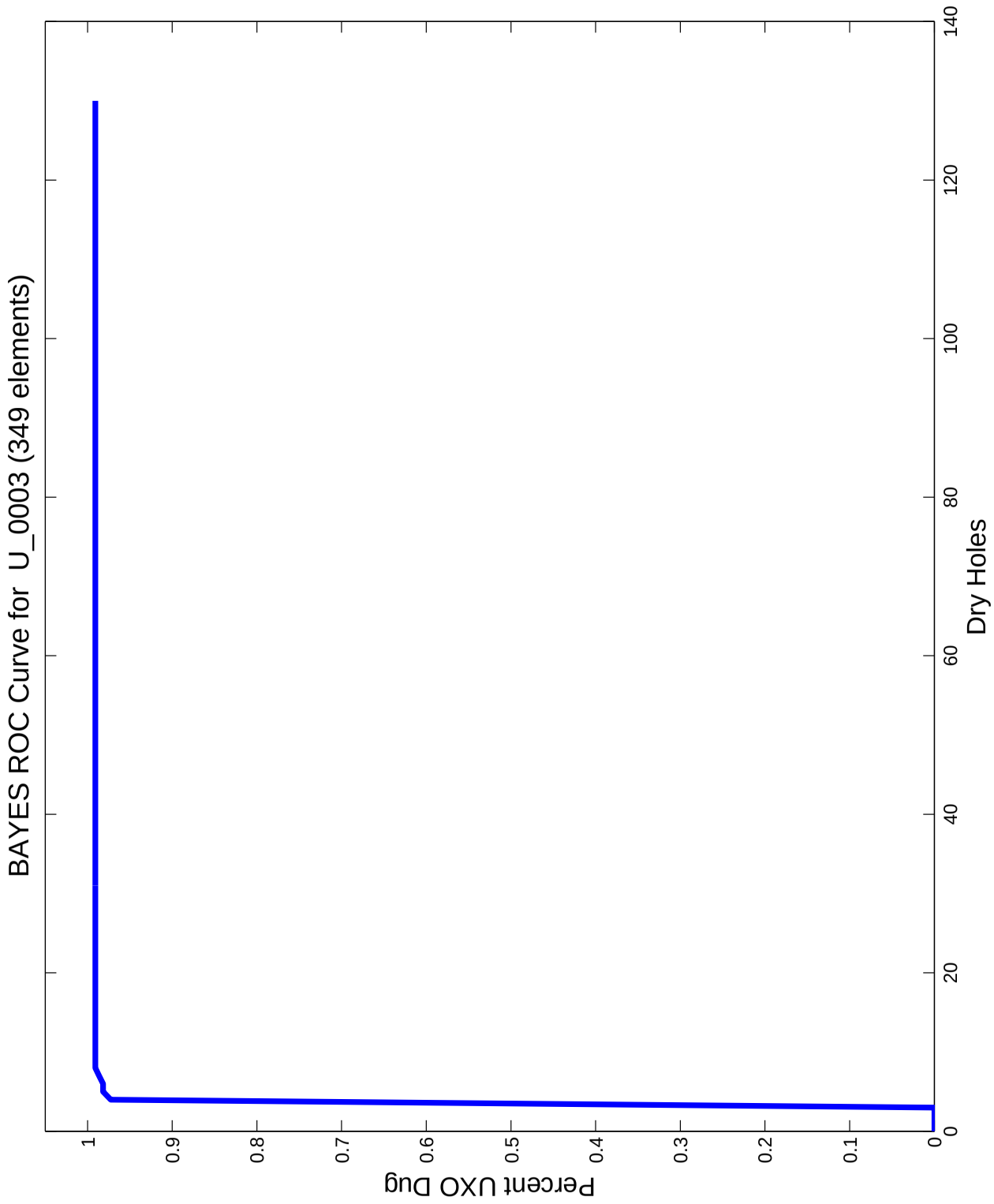

Figure 7: BAYESROC

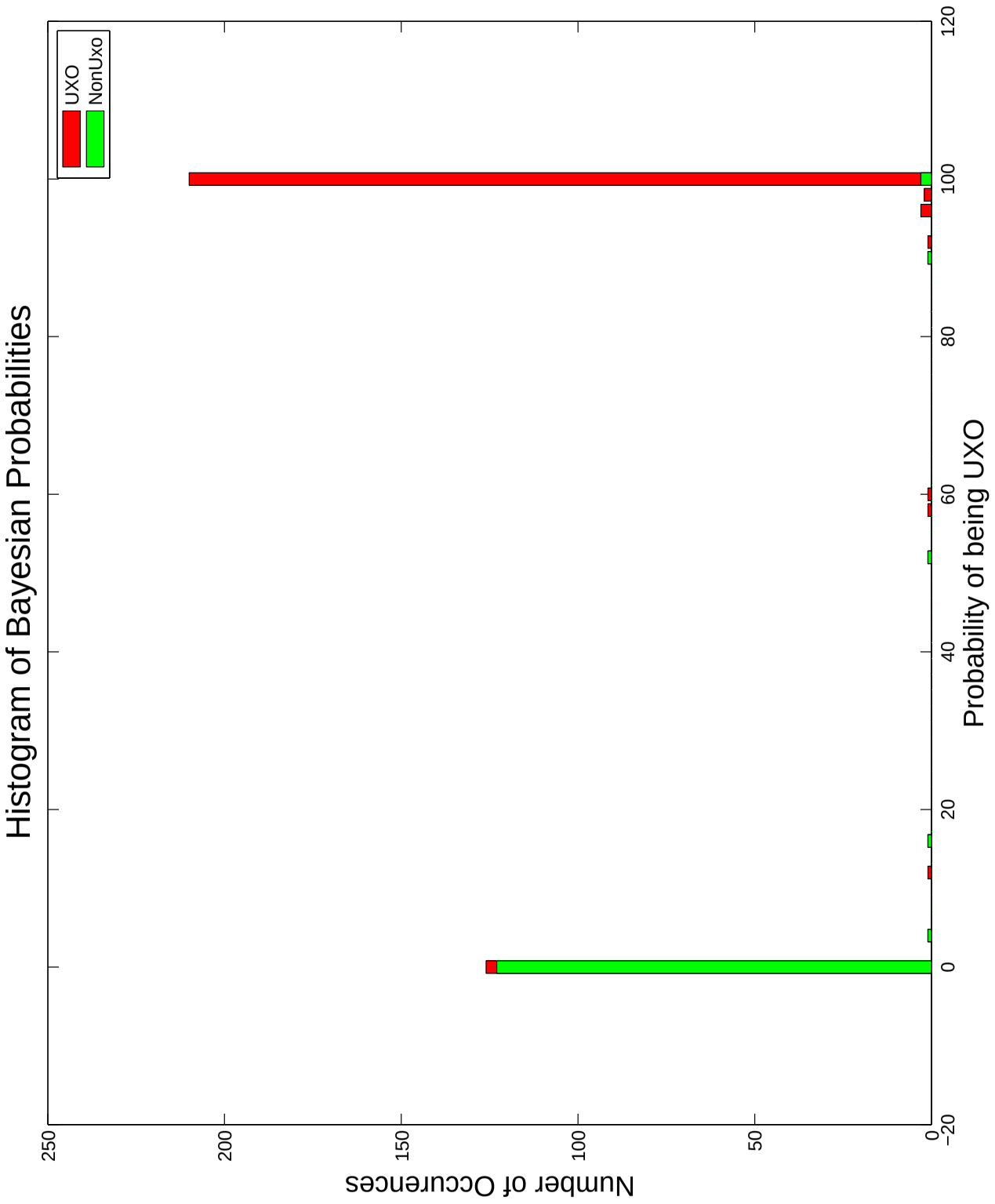

Figure 8: BAYESHISTO

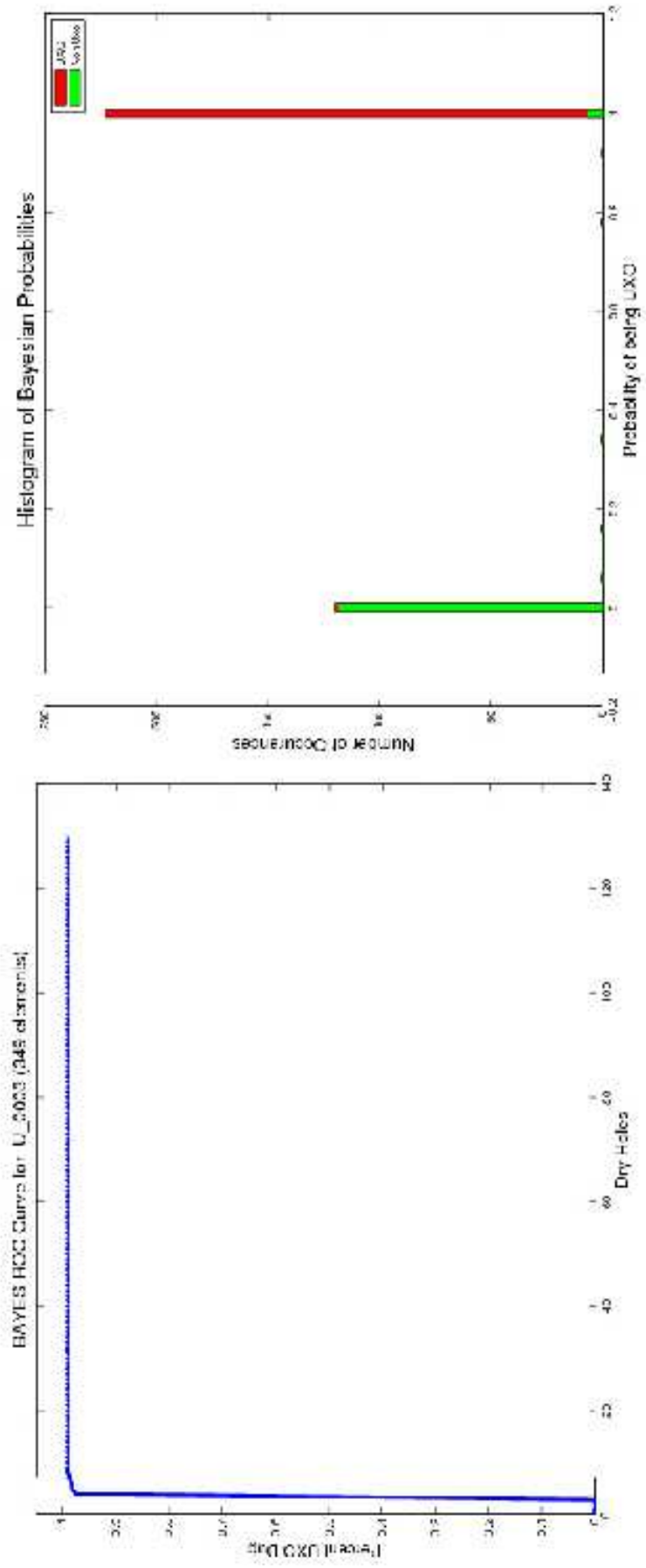

Figure 9: hybrid

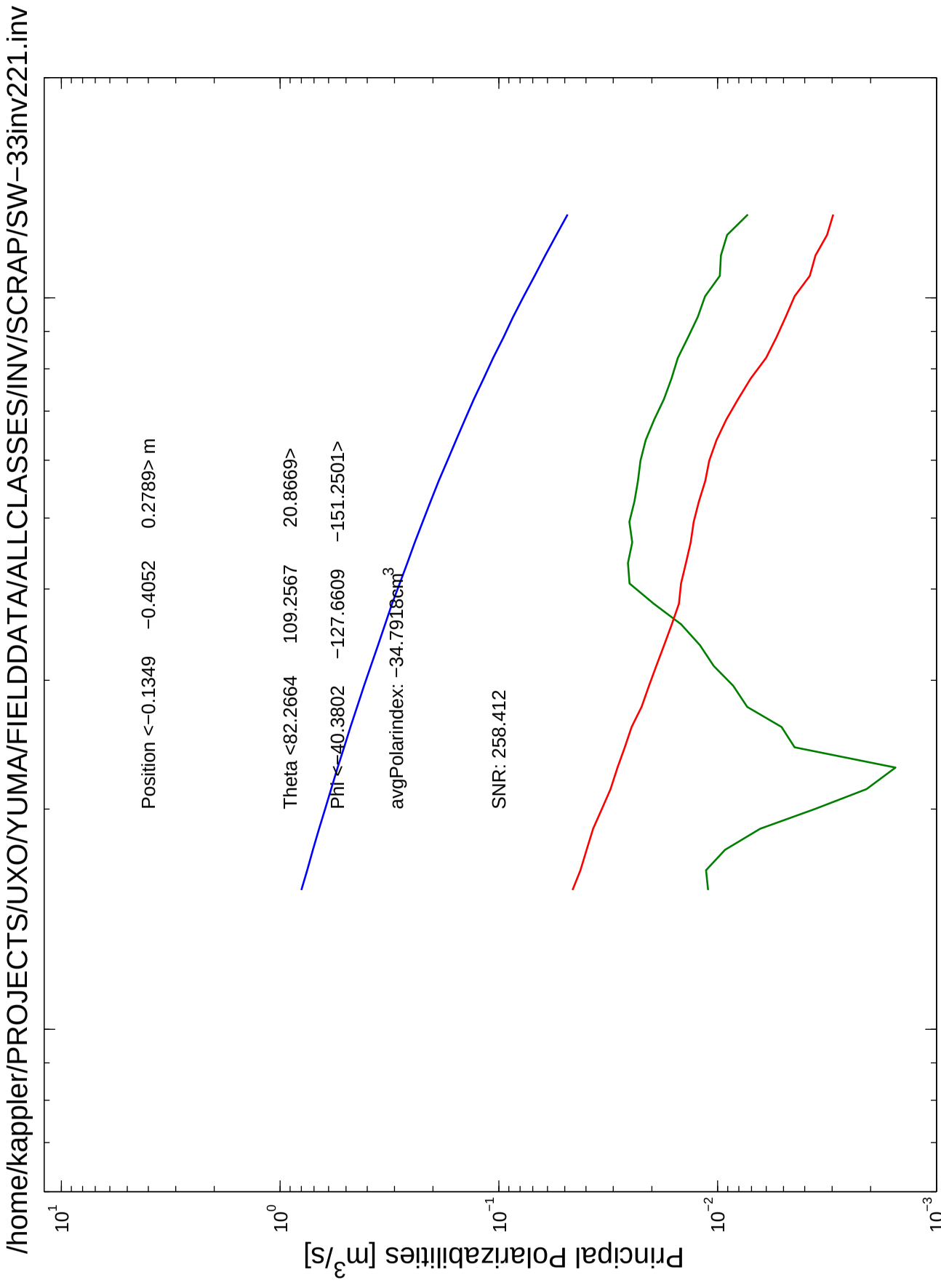

Figure 10: Scrap always classes as 37mm but with a big residual

stdDev of around 0.5 at most! So this thing is an outlier in every way except it always best fits the 37mm of all the trg data. **By the above, one can consider adding a test of observed residual w.r.t assumed class vs typical intraclass residual for the same class, but this mostly just saves you from a few FPs...**

References

[Butler, 2004] Butler, D., 2004, Report on a workshop on electromagnetic induction methods for UXO detection and discrimination: The Leading Edge, **23**, 766.

[Gasperikova et al., 2009] Gasperikova, E., J. Smith, H. Morrison, A. Becker, and K. Kappler, 2009, UXO detection and identification based on intrinsic target polarizabilities: A case history: Geophysics, **74**, B1.

[Kappler, 2008] Kappler, K., 2008, AN APPROACH TO UXO DISCRIMINATION VIA POLARIZABILITY CURVE-MATCHING AND FEATURE EXTRACTION APPLIED TO POLARIZABILITY CURVES: 'Proceedings of SAGEEP, Philadelphia, PA.

[Khadr et al., 1998] Khadr, N., B. Barrow, T. Bell, and H. Nelson, 1998, Target shape classification using electromagnetic induction sensor data: UXO Forum, Citeseer, 5–7.

[Morrison et al., 2005] Morrison, F., T. Smith, A. Becker, and E. Gasperikova, 2005, Detection and Classification of Buried Metallic Ob-

jects: Technical report, CALIFORNIA UNIV BERKELEY LAWRENCE BERKELEY LAB.

[Nelson et al., 2003] Nelson, H., B. Barrow, T. Bell, B. San Filipo, and I. Won, 2003, Characterization of a GEM-3 array for UXO classification: Proceedings of SPIE, 940.

[Pasion et al., 2008] Pasion, L., S. Billings, K. Kingdon, D. Oldenburg, N. Lhomme, and J. Jacobson, 2008, Cooperative Inversion of Time Domain Electromagnetic and Magnetometer Data for The Discrimination of Unexploded Ordnance: Journal of Environmental & Engineering Geophysics, **13**, 193.

[Pasion et al., 2007] Pasion, L., S. Billings, D. Oldenburg, and S. Walker, 2007, Application of a library based method to time domain electromagnetic data for the identification of unexploded ordnance: Journal of Applied Geophysics, **61**, 279–291.

[Pasion and Oldenburg, 2001] Pasion, L., and D. Oldenburg, 2001, A discrimination algorithm for UXO using time domain electromagnetics: Journal of Environmental and Engineering Geophysics, **6**, 91.

[Smith and Morrison, 2004] Smith, J., and H. Morrison, 2004, Estimating equivalent dipole polarizabilities for the inductive response of isolated conductive bodies: IEEE Transactions on Geoscience and Remote Sensing, **42**.

[Smith and Morrison, 2005] ———, 2005, Optimizing receiver configurations for resolution of equivalent dipole polarizabilities in situ: IEEE Transactions on Geoscience and Remote Sensing, **43**, 1490–1498.

[Smith et al., 2007] Smith, J., H. Morrison, L. Doolittle, and H. Tseng, 2007, Multi-transmitter multi-receiver null coupled systems for inductive detection and characterization of metallic objects: Journal of applied Geophysics, **61**, 227–234.

8 Appendix

HANDLE	Description	# Training Examples
UX106	105mm M456 HEAT	16
UX105	105mm M60	15
L1215	12 GAGE 15cm LOOP	4
L1230	12 GAGE 30cm LOOP	6
PUT12	12#SHOT	2
UX155	155mm M483A1	13
L1615	16 GAGE 15cm LOOP	5
L1630	16 GAGE 30cm LOOP	5
L1815	18 GAGE 15cm LOOP	4
L1830	18 GAGE 30cm LOOP	6
UX275	2.75in M230	13
L2015	20 GAGE 15cm LOOP	3
L2030	20 GAGE 30cm LOOP	3
UX020	20mm M55	15
SP030	30 CM STEEL PLATE	5
UX037	37mm	16
UX385	40mm M385	12
UXMK2	40mm MKII	13
UX057	57mm M86	13
SP060	60 CM STEEL PLATE	5
UX060	60mm M49A3	16
UX081	81mm M374	12
PUT08	8#SHOT	52
UXBDU	BDU-28	15
UXBLU	BLU-26	16
UXM42	M42	13
UXM75	M75	12
UX118	MK 118 ROCKEYE	15
SCRAP	scrap	41

Table 1: Training Classes

CLASS	fName	SNR	Est Depth	Notes
L2030	H16.inv	15.8166	0.5024	
PUT08	back5ew50.inv	1.1853	0.836	
PUT08	back6we51.inv	1.3105	0.8871	
SCRAP	ln0inv4.inv	22.7998	0.2311	
SCRAP	ln14qSE-36inv5.inv	170.143	0.3078	
SCRAP	ln15inv10.inv	223.73	0.2119	
SCRAP	ln36inv8.inv	43.4776	0.3499	
SCRAP	ln37inv7.inv	53.8824	0.2264	
SCRAP	ln40inv5.inv	327.375	0.2556	
SCRAP	ln5inv14.inv	712.826	0.2264	
SCRAP	ln5qSE-41inv11.inv	43.7198	0.2083	
SCRAP	ln61inv7.inv	25.0542	0.2664	
SCRAP	ln64inv6.inv	42.53	0.2373	
SCRAP	ln77inv16.inv	191.853	0.2547	
SCRAP	ln9inv8.inv	22.1736	0.345	
SCRAP	ln9inv9.inv	200.034	0.2082	
SCRAP	SE2-47inv4.inv	976.69	1.0225	
SCRAP	SE2-53inv56.inv	25.0039	0.2377	
SCRAP	SE2-59inv16.inv	135.577	0.2369	
SCRAP	SE2-60inv41.inv	932.396	0.2235	
SCRAP	SW-33inv221.inv	258.412	0.2789	
SCRAP	SW-34inv224.inv	20.7443	0.2	
SP060	F07.inv	152.722	1.2053	
SP060	flineinv6.inv	104.496	1.2699	
SP060	H07.inv	1444.9	0.6672	
SP060	hlineinv21.inv	633.286	0.7406	
SP060	hlineinv22.inv	527.164	0.7251	
UX020	m14ew9.inv	0.82058	2.8811	
UX057	k11ew15.inv	6.1095	2.6146	
UX057	m12ew13.inv	3.5398	2.8641	
UX060	k10ew17.inv	9.7147	2.028	
UX081	B02.inv	2.9742	1.245	
UX106	ilineinv19.inv	1.502	1.0819	
UX155	D04.inv	9.643	2.1373	
UX155	dlineinv9.inv	8.2991	2.2702	

Table 2: Troublesome Soundings